



Daily pan-evaporation estimation in different agro-climatic zones using novel hybrid support vector regression optimized by Salp swarm algorithm in conjunction with gamma test

Anurag Malik, Yazid Tikhamarine, Nadhir Al-Ansari, Shamsuddin Shahid, Harkanwaljot Singh Sekhon, Raj Kumar Pal, Priya Rai, Kusum Pandey, Padam Singh, Ahmed Elbeltagi & Saad Shauket Sammen

To cite this article: Anurag Malik, Yazid Tikhamarine, Nadhir Al-Ansari, Shamsuddin Shahid, Harkanwaljot Singh Sekhon, Raj Kumar Pal, Priya Rai, Kusum Pandey, Padam Singh, Ahmed Elbeltagi & Saad Shauket Sammen (2021) Daily pan-evaporation estimation in different agro-climatic zones using novel hybrid support vector regression optimized by Salp swarm algorithm in conjunction with gamma test, *Engineering Applications of Computational Fluid Mechanics*, 15:1, 1075-1094, DOI: [10.1080/19942060.2021.1942990](https://doi.org/10.1080/19942060.2021.1942990)

To link to this article: <https://doi.org/10.1080/19942060.2021.1942990>



© 2021 The Author(s). Published by Informa UK Limited, trading as Taylor & Francis Group



Published online: 02 Jul 2021.



[Submit your article to this journal](#)



Article views: 1241



[View related articles](#)







[View Crossmark data](#)



Citing articles: 12 [View citing articles](#)

Daily pan-evaporation estimation in different agro-climatic zones using novel hybrid support vector regression optimized by Salp swarm algorithm in conjunction with gamma test

Anurag Malik ^a, Yazid Tikhamarine^{b,c}, Nadhir Al-Ansari^d, Shamsuddin Shahid ^e, Harkanwaljot Singh Sekhon^f, Raj Kumar Pal^a, Priya Rai^g, Kusum Pandey^h, Padam Singh ⁱ, Ahmed Elbeltagi^j and Saad Shauket Sammen ^k

^aPunjab Agricultural University, Regional Research Station, Bathinda, Punjab, India; ^bSouthern Public Works Laboratory (LTPS), Tamanrasset, Algeria; ^cDepartment of Science and Technology, University Centre of Tamanrasset, Tamanrasset, Algeria; ^dCivil, Environmental and Natural Resources Engineering, Lulea University of Technology, Lulea, Sweden; ^eSchool of Civil Engineering, Faculty of Engineering, Universiti Teknologi Malaysia (UTM), Johor Bahru, Malaysia; ^fDepartment of Climate Change and Agricultural Meteorology, Punjab Agricultural University, Ludhiana, India; ^gDepartment of Soil and Water Conservation Engineering, College of Technology, G.B. Pant University of Agriculture and Technology, Pantnagar, Uttarakhand, India; ^hDepartment of Soil and Water Engineering, Punjab Agricultural University, Ludhiana, India; ⁱCollege of Forestry, Veer Chandra Singh Garhwali Uttarakhand University of Horticulture and Forestry, Ranichauri, Tehri Garhwal, Uttarakhand, India; ^jAgricultural Engineering Dept., Faculty of Agriculture, Mansoura University, Mansoura, Egypt; ^kDepartment of Civil Engineering, College of Engineering, Diyala University, Diyala 15 Governorate, Iraq

ABSTRACT

Ensuring accurate estimation of evaporation is weighty for effective planning and judicious management of available water resources for agricultural practices. Thus, this work enhances the potential of support vector regression (SVR) optimized with a novel nature-inspired algorithm, namely, Slap Swarm Algorithm (SVR-SSA) against Whale Optimization Algorithm (SVR-WOA), Multi-Verse Optimizer (SVR-MVO), Spotted Hyena Optimizer (SVR-SHO), Particle Swarm Optimization (SVR-PSO), and Penman model (PM). Daily EP (pan-evaporation) was estimated in two different agro-climatic zones (ACZ) in northern India. The optimal combination of input parameters was extracted by applying the Gamma test (GT). The outcomes of the hybrid of SVR and PM models were equated with recorded daily EP observations based on goodness-of-fit measures along with graphical scrutiny. The results of the appraisal showed that the novel hybrid SVR-SSA-5 model performed superior (MAE = 0.697, 1.556, 0.858 mm/day; RMSE = 1.116, 2.114, 1.202 mm/day; IOS = 0.250, 0.350, 0.303; NSE = 0.0861, 0.750, 0.834; PCC = 0.929, 0.868, 0.918; IOA = 0.960, 0.925, 0.956) than other models in testing phase at Hisar, Bathinda, and Ludhiana stations, respectively. In conclusion, the hybrid SVR-SSA model was identified as more suitable, robust, and reliable than the other models for daily EP estimation in two different ACZ.

ARTICLE HISTORY

Received 10 January 2021
Accepted 9 June 2021

KEYWORDS

Evaporation; Gamma test; Nature-inspired algorithms; Haryana; Punjab

1. Introduction

Evaporation is defined as the conversion of liquid water to water vapor due to the pressure difference between the earth-atmosphere system (Kim et al., 2015). Generally, the term evaporation states the loss of water in the form of vapors from the soil's surface. Pan-evaporation (EP) is an essential component of the hydrological cycle and is extensively used in scheming irrigation projects and provincial water resources (Azorin-Molina et al., 2015; Burn & Hesch, 2007). The evaporation rate is extremely high in arid and semiarid regions. Therefore, the accurate estimation of EP is vital for sustainable planning and management of water resources, particularly for irrigation practices, lakes and reservoir operations, water

budgeting, and studies related to hydrological modeling (Kisi & Heddam, 2019; Malik et al., 2017, 2020a; Moazen-zadeh et al., 2018; Rezaie-Balf et al., 2019; Seifi & Soroush, 2020). In addition, the system of agricultural practices like crop planning/ simulation and irrigation scheduling largely depends on the exact assessment of evaporation.

Generally, two approaches, (i) direct (i.e. pan-evaporimeter) and (ii) indirect (i.e. empirical or semi-empirical equations), are used for measuring the evaporation (Malik et al., 2020c). The direct EP estimation using Class A pan-evaporimeter has limited spatial coverage because of practical and instrumental problems (Shiri et al., 2014; Wang, Kisi, et al., 2017). In contrast, the application of the indirect EP estimation method,

CONTACT Anurag Malik  anuragmalik_swce2014@rediffmail.com

based on the relationship of ET with various climatic parameters, is often restricted due to data availability and climate variability (Ghaemi et al., 2019; Majidi et al., 2015). Considering the limitation of both the methods, the machine learning (ML) technique has been used in recent years as an alternative, such as SVR (support vector regression), MARS (multivariate adaptive regression splines), M5T (M5Tree), ELM (extreme learning machine), RF (random forest), MLP (multi-layer perceptron), GEP (gene expression programming), & ANFIS (adaptive neuro-fuzzy inference system). Besides, their hybrids with numerous algorithms enthused from nature have been effectively employed in pan-evaporation modeling (Ashrafzadeh et al., 2019; Guan et al., 2020; Seifi & Soroush, 2020; Shabani et al., 2020; Wu et al., 2020; Yaseen et al., 2020a).

Ghorbani et al. (2018) evaluated hybrid MLP-QPSO (quantum-behaved particle swarm optimization algorithm) against the hybrid MLP-PSO and simple MLP to forecast the daily EP rate at Talesh station of Iran. Results demonstrate that the hybrid MLP-QPSO provides better estimates than the other models. Feng et al. (2018) estimated monthly EP in temperate continental, temperate monsoon, mountain plateau, and subtropical monsoon zones of China utilizing ELM, ANN-PSO (artificial neural network), and ANN-GA (genetic algorithm) models. Results reveal that the ELM model outperformed the other models in all four climatic zones. Keshtegar et al. (2019) explored the potential of the SVR-RSM (response surface method) against the RSM, SVR, and MLP models for modeling monthly EP at six places in northeast Algeria. They found a better performance of the hybrid SVR-RSM model over other models. Allawi et al. (2020), Patle et al. (2020), Majhi et al. (2020), and Sebbar et al. (2019) applied various SCT (soft computing techniques) in different regions for predicting pan-evaporation. Their results endorse the feasibility of SCT.

Previous studies endorsed the feasibility of SCT in estimating EP from climate data. The studies also highlighted the scope of improvement of EP estimation methods. Evaporation is one of the most vital but complex meteorological variables. EP depends on several climatic factors, including temperature, solar radiation, humidity, sunshine hour, wind velocity, vapor pressure deficit, and albedo (Majhi & Naidu, 2021; Yaseen et al., 2020a). The influencing factors also depend on each other and various external factors (Wang et al., 2015). For example, vapor pressure deficit depends on air moisture content and air moisture-holding capacity, which again depends on air temperature. Therefore, the periodic variations and complexities of all influencing meteorological factors are integrated with EP (Wang et al., 2017). The dynamics of these meteorological variables and their complex

interactions make ET highly complex and nonlinear. The EP data often show high randomness and many outliers due to the large fluctuation of climatic variables (Su et al., 2015). Owing to the nonlinearity, complexity, and randomness in EP data, still need improvement in ML-based methods for precise estimation of ET.

One of the major challenges in EP estimation from meteorological variables using the ML algorithm is selecting input variables. The EP influencing variables significantly with time due to annual, seasonal, and random fluctuations of different meteorological variables (Pour et al., 2020). Thus, selecting the most appropriate variable for reliable EP estimation is a difficult task. The practice of the GT (Gamma test) for the selection of best inputs for ML models has received extensive attention in recent years (Ashrafzadeh et al., 2020; Das et al., 2019; Malik et al., 2018, 2020a, 2020c; Mohammadi et al., 2018; Singh et al., 2018). Rashidi et al. (2016) forecasted daily suspended sediment load (SSL) by optimizing the SVM (support vector machine) model with two kernel functions i.e. Radial Basis Function (RBF), and Polynomial in conjunction with GT in Korkorsar river (Iran). The GT and correlation analysis was performed to nominate the optimal combination of input for SSL modeling. The results of the investigation show that the GT-SVM with RBF kernel outperformed the other models. Choubin and Malekian (2017) applied ANN and ARIMA (autoregressive integrated moving average) models for predicting monthly groundwater level in the Shiraz basin, Iran. The optimal input combination and length of training and testing phases were decided by employing GT and M-test. They found better feasibility of the ARIMA model than the ANN model. They also reported that the GT can identify the most significant input variables with minimum effort and time for evaporation and SSL modeling.

The SVR has good generalization capability than many other ML algorithms (Malik et al., 2020d; Panahi et al., 2020). It is also highly robust to outliers (Borji et al., 2016; Qasem et al., 2019). Therefore, it is expected that SVR can provide a better estimation of pan-evaporation, which is highly complex and contains a large number of outliers. However, the performance of SVR, like other ML algorithms, depends on the optimization of its hyperparameters (Guan et al., 2020). The Salp swarm algorithm (SSA) is a recently developed metaheuristic optimizer conceptualized following the salps swarming mechanism (Mirjalili et al., 2017). The SSA has a powerful neighborhood search capability, making it highly efficient in finding global optima in a wide search space (Yaseen et al., 2020b). Therefore, a hybrid SVR model coupled with SSA was proposed for the enhancement of daily EP prediction capability in this research. The performance of the SVR-SSA was compared against the SVR-WOA, SVR-MVO,

SVR-SHO, SVR-PSO, and Penman model to evaluate the pan-evaporation prediction accuracy enhancement using the newly proposed algorithm. According to the authors' knowledge, so far, no study attempts to estimate pan-evaporation using the SVR model hybridized with the state-of-the-art metaheuristic optimization algorithm, SSA. The attempt to improve the prediction accuracy of pan-evaporation, one of the most complex but crucial hydrological variable, would contribute to the operation management of agricultural water resources in the context of growing water stress in agriculture due to global environmental changes.

2. Study location and climatic data collection

Three meteorological stations i.e. Hisar, Bathinda, and Ludhiana situated in two different agro-climates zones (ACZ) were considered under the present study. The detailed specification of geographical coordinates and climatic characteristics of study locations are listed in Table 1. The Bathinda and Ludhiana stations are placed in Punjab State, while Hisar station is located in Haryana State, India (see Figure 1). The mean annual rainfall is about 470, 436, and 660 mm at Hisar, Bathinda, and Ludhiana, respectively. The daily recorded climatic parameters of 4-years for Bathinda, Ludhiana, and Hisar Stations include pan-evaporation (EP, mm), solar radiation (R_s , MJ/m²/d), wind speed (U_s , km/h), maximum and minimum relative humidity (RH_{max} & RH_{min} , %), and minimum and maximum temperatures (T_{min} and T_{max} , °C) were obtained from meteorological observatories set up on Punjab Agricultural University-Regional Research Station (PAU-RRS), Bathinda, School of Climate Change and Agro-meteorology, PAU, Ludhiana, and Chaudhary Charan Singh Haryana Agricultural University, Hisar.

The statistical summary i.e. standard deviation (X_{STD}), skewness (X_{SKW}), kurtosis (X_{KUR}), minimum (X_{MIN}), maximum (X_{MAX}), and average (X_{AVG}) of T_{min} , T_{max} , RH_{max} , RH_{min} , U_s , R_s and EP for entire period are given in Table 2. It can be seen from Table 2, the climatic parameters ranges from $T_{min} = 0.8$ – 32.0 °C, $T_{max} = 9.2$ – 47 °C, $RH_{max} = 20.0$ – 100% , $RH_{min} = 6.0$ – 97.0% , $U_s = 0.0$ – 16.6 km/h, $R_s = 4.9$ – 28.0 MJ/m²/d, and EP = 0.0–20.0 mm/day at Bathinda, $T_{min} = 0.6$ – 34.5 °C, $T_{max} = 8.0$ – 45.8 °C, $RH_{max} = 22.0$ – 100% ,

Table 1. Location specifications and climatic characteristics for study locations.

Station	Latitude, N	Longitude, E	Elevation, m	Agro-climatic zone	Period
Hisar	29° 10' 00"	75° 46' 00"	215	Semi-arid	2011–2014
Bathinda	30° 17' 00"	74° 58' 00"	211	Semi-arid	2016–2019
Ludhiana	30° 54' 00"	75° 48' 00"	247	Sub-humid	2016–2019

Table 2. Statistics of measured daily climatic parameters at study stations.

Station/ dataset	Statistical factors	Climatic parameters						
		T_{min} (°C)	T_{max} (°C)	RH_{max} (%)	RH_{min} (%)	U_s (km/h)	R_s (MJ/m ² /d)	EP (mm)
Hisar								
Entire (2011–2014)	X_{MIN}	–1.500	8.000	25.000	9.000	0.000	5.000	0.200
	X_{MAX}	32.000	46.100	100.000	98.000	22.100	41.100	19.800
	X_{AVG}	16.789	30.768	83.029	46.666	4.851	17.378	4.445
	X_{STD}	8.652	7.786	15.459	18.685	3.033	5.443	3.076
	X_{SKW}	–0.193	–0.437	–1.151	0.597	1.213	–0.200	1.084
	X_{KUR}	–1.273	–0.473	0.603	–0.263	1.645	–0.574	1.084
Bathinda								
Entire (2016–2018)	X_{MIN}	0.800	9.200	20.000	6.000	0.000	4.900	0.000
	X_{MAX}	32.000	47.000	100.000	97.000	16.600	28.000	20.000
	X_{AVG}	17.211	31.048	79.778	49.819	2.372	15.816	6.623
	X_{STD}	8.185	7.662	14.595	17.554	2.515	5.874	4.490
	X_{SKW}	–0.251	–0.431	–1.084	0.002	2.052	–0.135	0.700
	X_{KUR}	–1.334	–0.529	0.858	–0.442	5.182	–0.942	–0.354
Ludhiana								
Entire (2016–2018)	X_{MIN}	0.600	8.000	22.000	5.000	0.000	4.800	0.000
	X_{MAX}	34.500	45.800	100.000	98.000	18.000	29.200	16.000
	X_{AVG}	18.062	30.076	80.979	46.618	3.637	16.723	4.327
	X_{STD}	8.072	7.467	16.068	18.914	2.551	6.602	2.968
	X_{SKW}	–0.198	–0.421	–1.249	0.285	1.561	–0.013	0.993
	X_{KUR}	–1.323	–0.521	0.641	–0.434	3.264	–0.974	0.292

where, X_{MIN} , X_{MAX} , X_{AVG} , X_{STD} , X_{SKW} , X_{KUR} are the minimum, maximum, average, standard deviation, skewness, and kurtosis of climatic parameters.

$RH_{min} = 5.0$ – 98.0% , $U_s = 0.0$ – 18.0 km/h, $R_s = 4.8$ – 29.2 MJ/m²/d, and EP = 0.0–16 mm/day at Ludhiana, and $T_{min} = -1.5$ – 32.0 °C, $T_{max} = 8.0$ – 46.1 °C, $RH_{max} = 25.0$ – 100% , $RH_{min} = 9.0$ – 98.0% , $U_s = 0.0$ – 22.1 km/h, $R_s = 5.0$ – 41.1 MJ/m²/d, and EP = 0.2–19.8 mm/day at Hisar, respectively. Also, the X_{SKW} was noted negative, and positive, while platykurtic and leptokurtic feature were recorded through X_{KUR} at study places.

The obtained daily climatic data of 4-years was separated into two groups (i) training group (75%: 01–01–2016–31–12–2018 for Bathinda and Ludhiana stations, and 01–01–2011–31–12–2013 for Hisar station), and (ii) testing group (25%: 01–01–2019–31–12–2019 for Bathinda and Ludhiana stations, and 01–01–2014–31–12–2014 for Hisar station) to enhance the proposed models.

3. Methodology

3.1. Gamma test

The GT was employed to identify the most appropriate input combinations that influence the evaporation rate at three study locations. GT compute the MSE (minimum square error) in continuous nonlinear models with unseen observations and was first introduced by Stefánsson et al. (1997). Present-day, the extensive application of GT has been found in water resources engineering (Borji et al., 2016; Choubin & Malekian, 2017; Malik et al.,

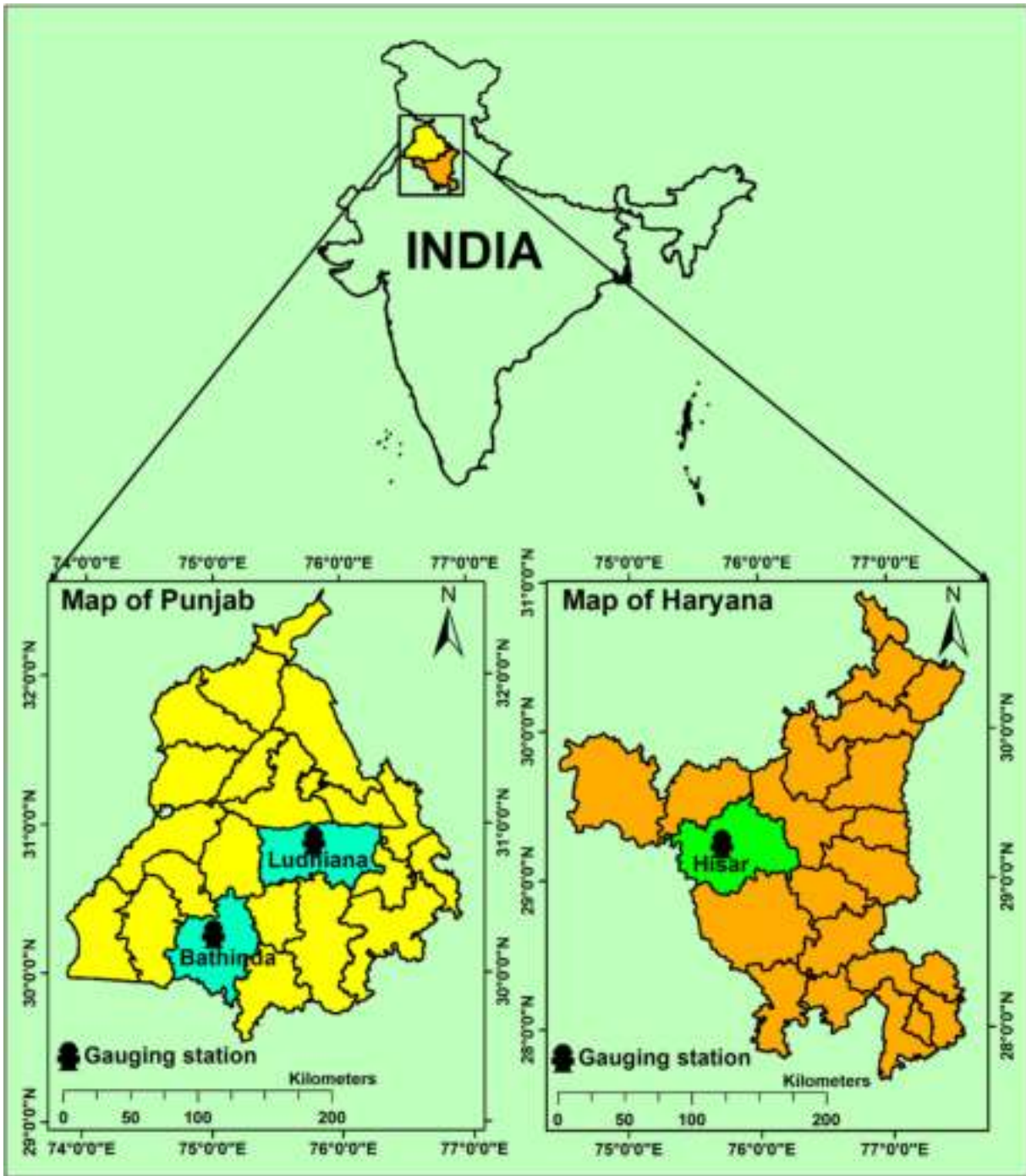


Figure 1. Geographical specifications of study stations, India.

2020c, 2020a; Seifi & Riahi, 2020; Singh et al., 2018). The association among the inputs (x) and output (y) variables is defined by Eq. (1):

$$y = Gx + \Gamma \quad (1)$$

In which, G and Γ represent the gradient and intercept of the line of regression ($x = 0$), and y defines the output. For model development, the output of Eq. (1) is

very appreciated. G and Γ with small values designate the more appropriate input variables. One more, indicator i.e. V-Ratio ($VR = \Gamma/(\sigma^2(y))$), here, Γ is the gamma function, and $\sigma^2(y)$ is the output variance, employed widely for nominating the optimal input parameters. In the present work, the appropriate input combination for hybrid SVR models was finalized based on the minimum value of Γ , G , and VR (Malik et al., 2017; Piri et al., 2009).

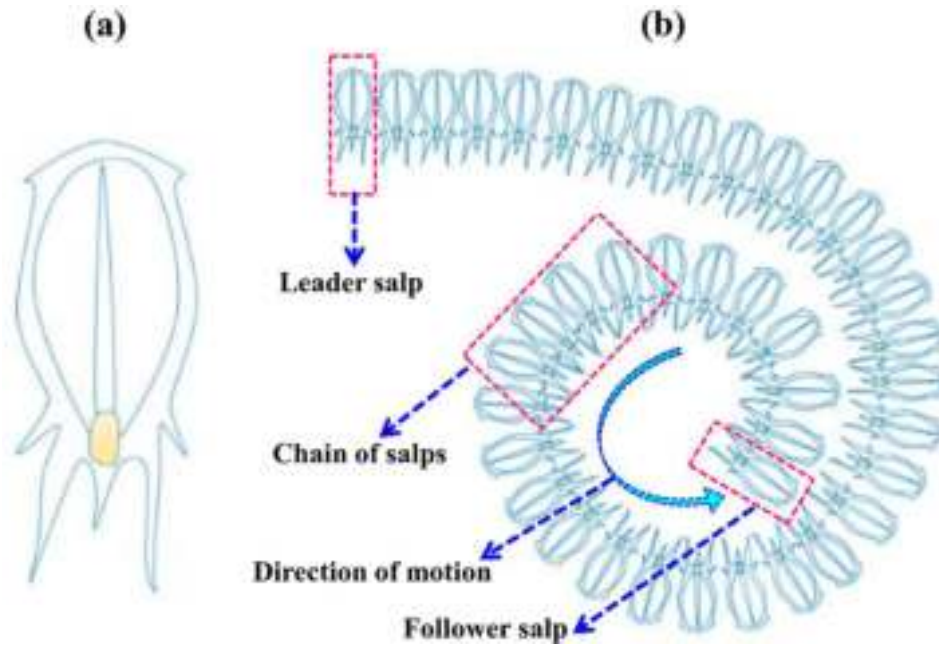


Figure 2. Illustration of (a) individual salp, and (b) Chain of salps (Yaseen et al., 2020b).

3.2. Support vector regression

Usually, two versions of SVM, i.e. SVR and SVC (support vector classifier) are available to solve the multi-optimization problems. SVR, a new artificial intelligence technique, was proposed by Vapnik (1995), employed minimization of structural risk code from statistical learning theory. SVM can reduce error during all modeling stages to obtain a functional dependency that has the most deviation of all training data from the original target vectors and should be as linear as possible (Smola & Scholkopf, 1998). The accuracy of SVR depends greatly on the correct selection of three hyperparameters (i) penalty constant (C), (ii) kernel function (γ), and (iii) tube size (ϵ). The parameter C controls the complexity of the model or manage the margin maximization and error minimization during the training stage. The small value of the C parameter means the maximized margin without overfitting (Keerthi & Lin, 2003; Rashidi et al., 2016). The ϵ parameter refers to the insensitivity, i.e. the number of deviations tolerated by the SVR during the process of regression (Jajarmizadeh et al., 2015; Kakaei Lafdani et al., 2013). The γ is the kernel function parameter and panels the classification accuracy of the model, or in other words, control the overfitting and underfitting in the network (Tharwat & Hassanien, 2018). Thus, a small value of γ leads to underfitting and vice-versa (Cui et al., 2020; Rashidi et al., 2016). Therefore, several experiments must be carried out to obtain optimal results.

In the present research, several trials were led to attaining the finest values of C , γ (with radial basis function), ϵ parameters computed using nature-inspired algorithms. More details about the theory and formulation of SVR

can be obtained from Vapnik (1995), Gunn (1998), and Panahi et al. (2020).

3.3. Nature-inspired algorithms

3.3.1. Salp swarm algorithm

Recently, a new optimization algorithm, i.e. SSA, was created by Mirjalili et al. (2017). The SSA algorithm simulates the behavior of marine animals known as salps. In deeding oceans, salps generally form a swarm called Salp series or Salp chains. The Salp chains are fragmented into (i) leader and (ii) follower. The leader should be at the front of the chain and the other salp will follow the leader in the chain shape, as mentioned in Figure 2 (Yaseen et al., 2020b). Just like other optimization algorithms, SSA balances capabilities between exploration and exploitation to achieve an optimal solution and avoid trapping in the optimal local solution using the following equations:

$$Z_n^1 = \begin{cases} P_n + r_1((u_n - l_n)r_2 + l_n) & r_3 \geq 0 \\ P_n - r_1((u_n - l_n)r_2 + l_n) & r_3 < 0 \end{cases} \quad (2)$$

where, Z_n^1 denotes the location of the leader in the n^{th} dimension, P_n denotes the location of food exporter in the n^{th} dimension, u_n denotes the upper limit of n^{th} dimension, l_n denotes the lower limit of n^{th} dimension, r_1, r_2, r_3 are random coefficients (0, 1). The coefficient r_1 is the most crucial in SSA balances the abilities of the exploration and exploitation using Eq. (3):

$$r_1 = 2e^{-\left(-\frac{4a}{A}\right)^2} \quad (3)$$

Here, A and a express the maximum and current iterations. The supporters are transferred from the first location to another one using Eq. (4):

$$Z_n^m = \frac{1}{2}ce^2 + v_0e \quad (4)$$

In which, $m \geq 2$, Z_n^m describes the position of the i^{th} follower salp in j^{th} dimension, e outlines time, v_0 states the initial speed, and $c = \frac{v_{\text{final}}}{v_0}$ where, $v = \frac{Z-Z_0}{e}$.

3.3.2. Particle swarm optimization

PSO is one of the most swarm intelligent algorithm exploited to solve optimization problems (Kennedy & Eberhart, 1995). It entused their basic concept from the behaviors of bird flocks. The PSO could be used in different fields of optimization, such as multiple-objective optimization, nonlinear and stochastic problems (Malik et al., 2020d; Tikhamarine et al., 2019, 2020). The working assembly of PSO could be summarized in the following steps:

- (1) Firstly, the searching area should be specified using a group of possible stochastic solutions.
- (2) Estimate the feasibility of each particle in the swarm.
- (3) In each iteration, make a comparison between the expediency of each particle with their expediency obtained in the previous iteration.
- (4) Compare the expediency of particles with each other and obtain the global best position with the super expediency.
- (5) Update the velocity of all particles according to their expediency.
- (6) Repeat Steps 2–5 until the design criteria are achieved.

More information, including theories and applications about using the PSO algorithm, can be found in Kennedy and Eberhart (1995).

3.3.3. Spotted hyena optimizer

Dhiman and Kumar developed the Spotted Hyena Optimizer (SHO) algorithm (2017), simulating the social behavior of spotted hyenas in nature and how they hunt the prey. The hunting mechanisms are based on four main steps (i) encircling, (ii) hunting, (iii) attacking prey, and (iv) research for prey. Readers, for more details, theories, and applications of SHO refers to Dhiman and Kumar (2017, 2019).

3.3.4. Whale optimization algorithm

Mirjalili and Lewis (2016) presented WOA (whale optimization algorithm), one of the modern meta-heuristic techniques inspired by the chase method followed by

humpback whales to hunt prey. The WOA employs a community of exploring agents to find the optimum solution for optimizing problems. As in most optimization algorithms, the searching procedure begins with several random solutions for the specific problem. Then these random solutions are iteratively improved until the optimum solution is obtained. For further about the theories and applications of the WOA algorithm, readers can refer to Mirjalili and Lewis (2016), Al-Zoubi et al. (2018), Elaziz and Mirjalili (2019), Heidari et al. (2020), and Mirjalili et al. (2020).

3.3.5. Multi-verse optimizer

Mirjalili et al. (2016), based on WH (white hole), BH (black hole), and WH (wormhole) concepts, presented the MVO (multi-verse optimizer) algorithm to describes three phases viz. exploration, exploitation, and local search, respectively. For more details about the theory, and application of the MVO algorithms, obtain from Mirjalili et al. (2016) and Aljarah et al. (2020).

3.4. Penman model

Penman model (Penman, 1948) was utilized for determining the rate of evaporation by using climatic variables at three study locations in this study, and expressed as:

$$EP = \frac{\Delta R_n + \gamma E_a}{\Delta + \gamma} \quad (5)$$

In Eq. (5) EP (mm/day) = evaporation rate, Δ (kPa/°C) = slope of saturation vapor pressure-air temperature curve, R_n (MJ/m²/day) = net radiation, γ = psychrometric constant (kPa/°C), and E_a = aerodynamic function (mm/day), and calculated as $E_a = f(u) \times (e_s - e_a)$, in which e_s and e_a are the saturation and actual vapor pressure (kPa), and $f(u)$ is the theoretically derived aerodynamic wind function and computed as $f(u) = 0.263(a_w - b_w u_s)$, in which a_w and b_w are empirical coefficients ($a_w = 0.5$ and $b_w = 0.537$) proposed for open water bodies by Penman (1956), and u_s = wind speed at 2 elevation (m/s). The R_n , Δ , γ , e_s and e_a are computed by using the method given by Allen et al. (1998) in FAO-56 (Food and Agriculture Organization) manual.

3.5. Integrated hybrid SVR models and goodness-of-fit measures

The SVR constraints are required to determine wisely to achieve the robust performance of SVR models. Five nature-inspired algorithms, including SSA, SHO, PSO, WOA, and MVO, were integrated with the SVR model to define the three responsible parameters (i.e. C, γ , and ϵ) for SVR performance. The accuracy of these

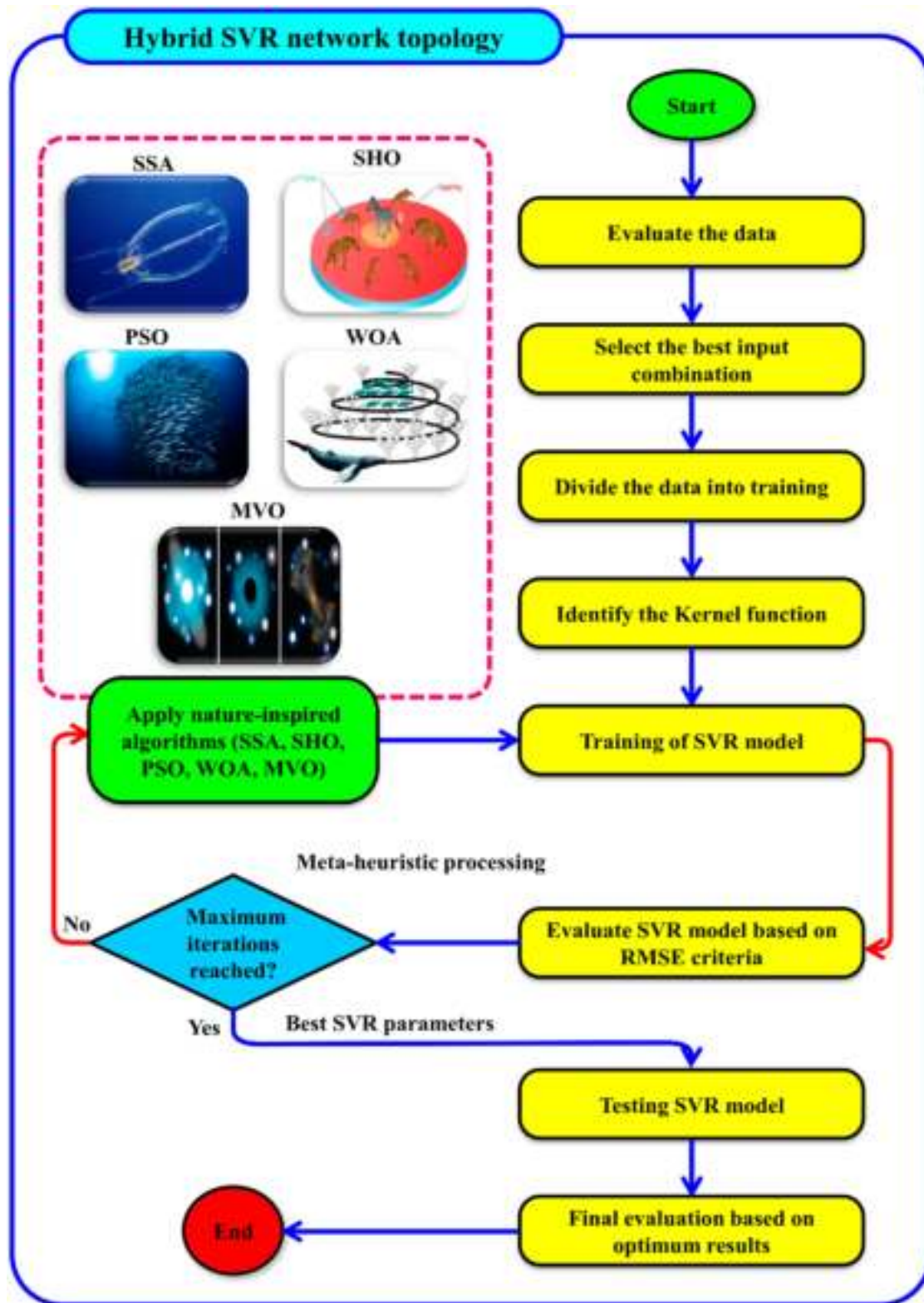


Figure 3. Topology of proposed hybrid SVR models for daily EP estimation at study stations.

hybrid SVR models largely depends on the choice of three responsible parameters, i.e. C , γ , and ϵ , which help find the global optimal solution by counting the minimum possible error within the expected and target variable

quantity. The lowest value of RMSE during the training state was considered for the assessment of these algorithms. The search range for SVR parameters (i.e. C , ϵ , and γ) are examined in the exponential planetary [$C \in$

(10–5, 105), $\gamma \in (0, 101)$ and $\gamma \in (0, 101)$] for this study. Figure 3 demonstrates the flowcharts of the constructed hybrid SVR models coupled with five nature-inspired algorithms, i.e. WOA, SHO, SSA, PSO, MVO in semiarid and sub-humid regions for daily EP estimation.

The performance of constructed hybrid SVR and PM were evaluated through goodness-of-fit measures (i.e. NSE: Nash-Sutcliffe efficiency, MAE: mean absolute error, PCC: Pearson correlation coefficient, RMSE: root mean square error; IOA: index of agreement, & IOS: index of scattering), and by pictorial examination (i.e. Taylor diagram, radar-chart, temporal plots). The MAE (Elbeltagi et al., 2020; Rehamnia et al., 2021), RMSE (Abba et al., 2021; Malik et al., 2021a; Pandey et al., 2020), IOS (Malik et al., 2019; Tao et al., 2018), NSE (Nash & Sutcliffe, 1970), PCC (Malik et al., 2020b, 2021b), and IOA (Tikhamarine et al., 2020; Willmott, 1981) are stated as:

$$MAE = \frac{1}{N} \sum_{i=1}^N |EP_{est,i} - EP_{obs,i}|$$

$$(0 < MAE < \infty) \quad (6)$$

$$RMSE = \sqrt{\frac{1}{N} \sum_{i=1}^N (EP_{obs,i} - EP_{est,i})^2}$$

$$(0 < RMSE < \infty) \quad (7)$$

$$IOS = \frac{\sqrt{\frac{1}{N} \sum_{i=1}^N (EP_{obs,i} - EP_{est,i})^2}}{\overline{EP_{obs}}}$$

$$(0 < IOS < \infty) \quad (8)$$

$$NSE = 1 - \left[\frac{\sum_{i=1}^N (EP_{obs,i} - EP_{est,i})^2}{\sum_{i=1}^N (EP_{obs,i} - \overline{EP_{obs}})^2} \right]$$

$$(-\infty < NSE < 1) \quad (9)$$

$$PCC = \frac{\sum_{i=1}^N (EP_{obs,i} - \overline{EP_{obs}}) (EP_{est,i} - \overline{EP_{est}})}{\sqrt{\sum_{i=1}^N (EP_{obs,i} - \overline{EP_{obs}})^2 \times \sum_{i=1}^N (EP_{est,i} - \overline{EP_{est}})^2}}$$

$$(-1 < PCC < 1) \quad (10)$$

$$IOA = 1 - \left[\frac{\sum_{i=1}^N (EP_{est,i} - EP_{obs,i})^2}{\sum_{i=1}^N (|EP_{est,i} - \overline{EP_{obs}}| + |EP_{obs,i} - \overline{EP_{obs}}|)^2} \right]$$

$$(0 < IOA \leq 1) \quad (11)$$

Note: N defines the number of observations, EP_{obs} , and EP_{est} outlines i^{th} observations of recorded (observed) and estimated daily EP. $\overline{EP_{obs}}$ and $\overline{EP_{est}}$ explain the mean of daily EP for recorded and estimated values. The best

model was nominated based on least MAE, RMSE, IOS values, higher NSE, PCC, and IOA values in testing for daily EP estimation at study locations.

4. Results

4.1. Nomination of optimal inputs with GT

The assortment of an optimal set of inputs is important for the performance of the prediction model. Different combinations of inputs were used in hybrid-SVR models for the selection of an optimal set of inputs. In this study, five combinations of six input variables (T_{\min} , T_{\max} , RH_{\max} , RH_{\min} , U_s , R_s) were tested, as elaborated in Table 3. The GT was employed to assess the relative performance of different input combinations to select the best combination for developing the EP prediction model. The obtained results in three study locations are presented in Table 4. The values of three GT statistics (Γ , G , and VR) for all the five input combinations at all three locations are provided in Table 4. The *Mask* (the last column of Table 4) is used to show the input combination. As six variables were considered in this study

Table 3. Input parameters of hybrid SVR models optimized by five nature-inspired algorithms for study stations.

Climatic parameters	Optimized SVR model by WOA, SHO, SSA, PSO, and MVO algorithms				
	1	2	3	4	5
T_{\min} (°C)				✓	✓
T_{\max} (°C)	✓	✓	✓	✓	✓
RH_{\max} (%)			✓		✓
RH_{\min} (%)					✓
U_s (km/h)		✓	✓		✓
R_s (MJ/m ² /d)				✓	✓

Table 4. GT results on different input combination at study stations.

Model	Combination	GT statistics			
		Γ	G	VR	Mask
Hisar					
1	T_{\max}	0.062	0.628	0.249	010000
2	T_{\max} , U_s	0.040	0.368	0.160	010010
3	T_{\max} , RH_{\max} , U_s	0.041	0.045	0.166	011010
4	T_{\min} , T_{\max} , R_s	0.046	0.548	0.183	110001
5	T_{\min} , T_{\max} , RH_{\max} , RH_{\min} , U_s , R_s	0.036	0.019	0.144	111111
Bathinda					
1	T_{\max}	0.076	0.742	0.306	010000
2	T_{\max} , U_s	0.064	0.493	0.254	010010
3	T_{\max} , RH_{\max} , U_s	0.052	0.110	0.207	011010
4	T_{\min} , T_{\max} , R_s	0.062	0.170	0.249	110001
5	T_{\min} , T_{\max} , RH_{\max} , RH_{\min} , U_s , R_s	0.039	0.046	0.156	111111
Ludhiana					
1	T_{\max}	0.057	0.446	0.228	010000
2	T_{\max} , U_s	0.039	0.245	0.156	010010
3	T_{\max} , RH_{\max} , U_s	0.036	0.036	0.143	011010
4	T_{\min} , T_{\max} , R_s	0.041	0.316	0.165	110001
5	T_{\min} , T_{\max} , RH_{\max} , RH_{\min} , U_s , R_s	0.027	0.030	0.110	111111

to select inputs, the *Mask* is presented using six digits correspond to six variables, T_{\min} , T_{\max} , RH_{\max} , RH_{\min} , U_s , R_s . Digit '1' indicates the input is used while '0' indicates the input is not used. Therefore, '010000' indicates only T_{\max} is used as input while '111111' indicates all the meteorological variables are used as input.

The performance of an input combination is considered better if it provides lower values of GT statistics. The results presented in Table 4 show a gradual decrease of Γ and VR values with the increase of inputs at all three locations. A fluctuation of G values with the increase of inputs was noticed. However, it also showed the lowest values at all the stations for the fifth input combination where all the meteorological variables were considered as input. The results indicate the influence of all the meteorological variables on EP in the study area. Thus, information of all the variables is required for reliable estimation of EP in the study area.

4.2. Daily EP estimation in two different agro-climatic zones

The EP estimation models were developed by hybridizing the SVR with five optimization algorithms, WOA, SHO, SSA, PSO, MVO. The models were termed as SVR-PSO-5, SVR-WOA-5, SVR-SSA-5, SVR-SHO-5, and SVR-MVO-5 in this study, where 5 indicates the fifth input combination (presented in Table 3). The models were calibrated with 75% of daily observed data and validated for the rest 25% data. The act of the hybrid models was compared with the PM, which is most widely used globally to estimate EP. The performance of the models

was evaluated using both goodness-of-fit measures (or statistical metrics) and graphical presentations.

In terms of six statistical indices, the model's performance during validation is presented in Table 5. The statistical metrics are also presented using the radar chart in Figure 4(a-c). All five hybrid models performed much better than the Penman method in estimating EP in terms of all the six statistics at all three locations. The relative performance of the hybrid models revealed their similar performances. The radar chart shows that the performance lines of all five models overlap each other, indicating the close performance of the models with each other. However, a closer observation of the statistics revealed a bit better performance of the SVR-SSA-5 model than the other applied models. The performance measures i.e. MAE, RMSE, IOS, NSE, PCC, and IOA values for SVR-SSA-5 were 0.697, 1.116, 0.250, 0.861, 0.929 and 0.960 at Hisar, 1.556, 2.114, 0.350, 0.750, 0.868 and 0.925 for Bathinda, and 0.858, 1.202, 0.303, 0.834, 0.918 and 0.956 for Ludhiana. The low values of MAE, RMSE, and IOS and near to ideal NSE, PCC, and IOA values at all three locations indicate an excellent concert of the SVR-SSA-5 model in the estimation of daily EP from meteorological variables. The performance of SVR improved with SHO, WOA, PSO, and MVO corresponding to input combination 5 and Penman model was found inconsistent at different locations. For example, SVR-WOA-5 showed better performance at Hisar and Ludhiana, while SVR-SHO-5 showed better performance at Bathinda. Therefore, it was not possible to rank these two models based on the used statistical indices.

Table 5. Goodness-of-fit measures of hybrid SVR models during testing at study stations.

Station/model	Optimal parameters			Goodness-of-fit measures					
	γ	C	ϵ	MAE (mm/day)	RMSE (mm/day)	IOS	NSE	PCC	IOA
Hisar									
SVR-WOA-5	2.676E-04	122.901	1.180E+02	0.699	1.121	0.252	0.859	0.928	0.960
SVR-SHO-5	4.275E-03	2.623	2.539E-03	0.750	1.266	0.284	0.821	0.907	0.948
SVR-SSA-5	1.028E-04	999.876	1.000E-01	0.697	1.116	0.250	0.861	0.929	0.960
SVR-PSO-5	1.896E-07	998.148	4.684E-02	0.937	1.493	0.335	0.751	0.870	0.920
SVR-MVO-5	1.246E-08	997.578	1.693E-02	1.114	1.762	0.395	0.652	0.829	0.870
Penman	/	/	/	1.726	2.261	0.507	0.428	0.727	0.690
Bathinda									
SVR-WOA-5	2.382E-08	986.726	9.867E-02	1.693	2.258	0.374	0.715	0.849	0.912
SVR-SHO-5	9.403E-04	0.154	1.047E-03	1.610	2.179	0.361	0.735	0.862	0.916
SVR-SSA-5	4.587E-03	0.441	1.255E-06	1.556	2.114	0.350	0.750	0.868	0.925
SVR-PSO-5	1.742E-07	235.024	2.901E-02	1.691	2.256	0.374	0.716	0.849	0.912
SVR-MVO-5	1.470E-08	998.246	2.291E-02	1.808	2.348	0.389	0.692	0.844	0.889
Penman	/	/	/	2.913	4.161	0.689	0.032	0.598	0.562
Ludhiana									
SVR-WOA-5	5.862E-07	996.125	2.146E-01	0.925	1.250	0.315	0.820	0.909	0.951
SVR-SHO-5	1.524E-04	0.121	6.920E-03	0.936	1.317	0.332	0.801	0.898	0.938
SVR-SSA-5	5.001E-06	994.252	1.526E-01	0.858	1.202	0.303	0.834	0.918	0.956
SVR-PSO-5	1.756E-07	996.246	5.481E-02	0.951	1.290	0.325	0.809	0.902	0.947
SVR-MVO-5	2.457E-08	997.543	6.286E-02	1.002	1.357	0.342	0.788	0.893	0.932
Penman	/	/	/	1.993	2.559	0.645	0.247	0.500	0.575

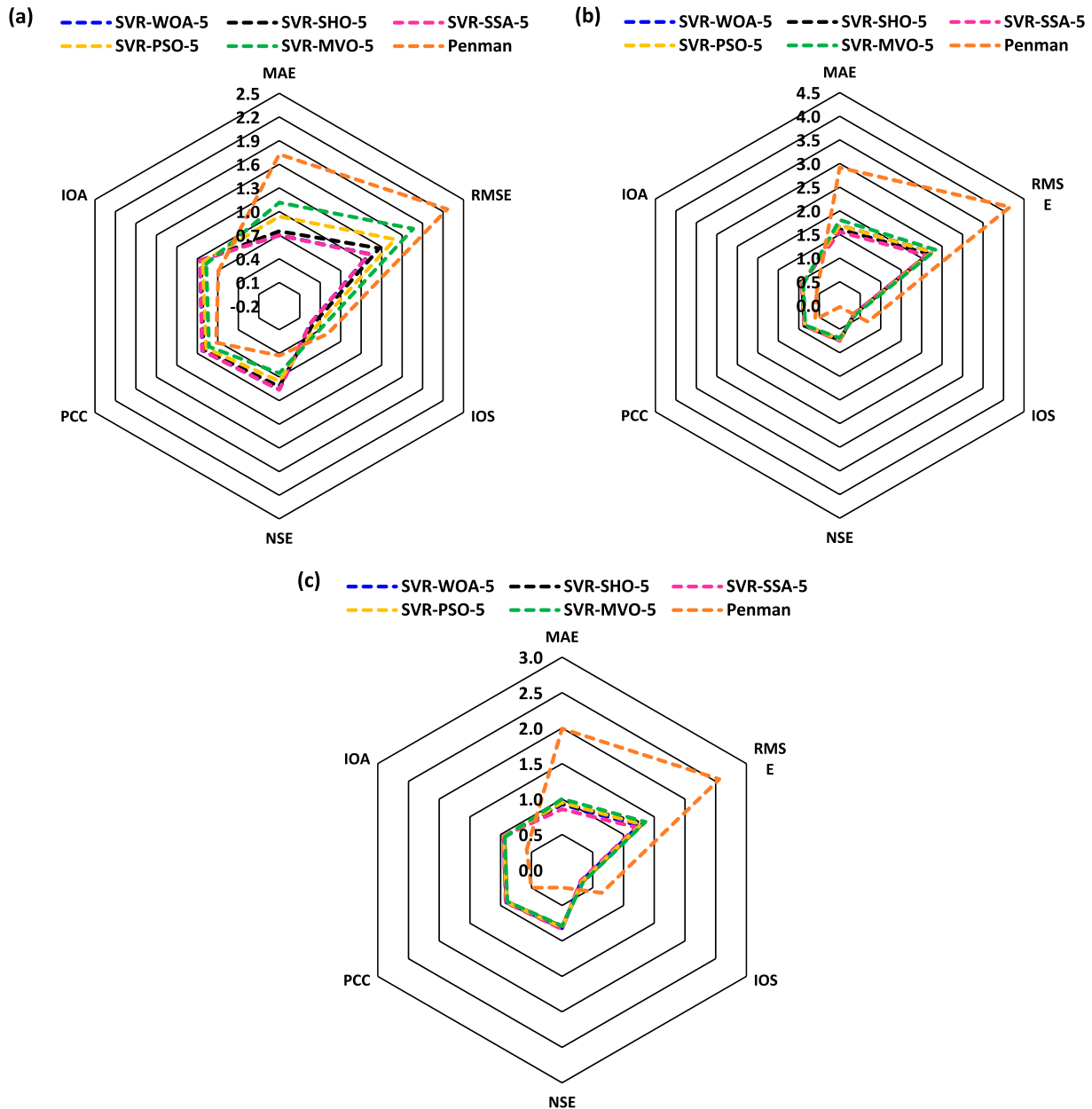


Figure 4. Radar charts display the goodness-of-fit measures of SVR-WOA-5, SVR-SHO-5, SVR-SSA-5, SVR-PSO-5, SVR-MVO-5, and PM models during testing at (a) Hisar, (b) Bathinda, and (c) Ludhiana stations.

The temporal difference of observed and estimated daily EP values during testing at different stations is presented in Figures 5–7 (a–f). The time series of observed and estimated EP by the hybrid models showed a good match at all the stations. Penman method A showed a large underestimation of EP values. The hybrid models also underestimated the extremely high EP values and overestimated the extremely low values. The under- and over-estimation were more at Bathinda station, where data is much noisy. However, all the hybrid models were able to replicate the seasonal variability and most of the daily fluctuations of EP reliably.

The scatter plots are presented in the right panel of Figures 5 (a–f) to 7 (a–f). The best fit lines of the estimated EP by the hybrid models against the observed EP were very close to the diagonal line of the plots at all the stations. The determination coefficient (R^2) values for SVR-WOA-5 models at Hisar, Bathinda and Ludhiana were 0.862, 0.721 and 0.827, while those were 0.823, 0.743 and 0.807 for SVR-SHO-5 model, 0.863, 0.753 and 0.842 for SVR-SSA-5 model, 0.756, 0.721 and 0.813 for SVR-PSO-5 model, 0.688, 0.713 and 0.798 for SVR-MVO-5 model, and 0.528, 0.358 and 0.250 for Penman model, respectively. The lower performance of all the models was

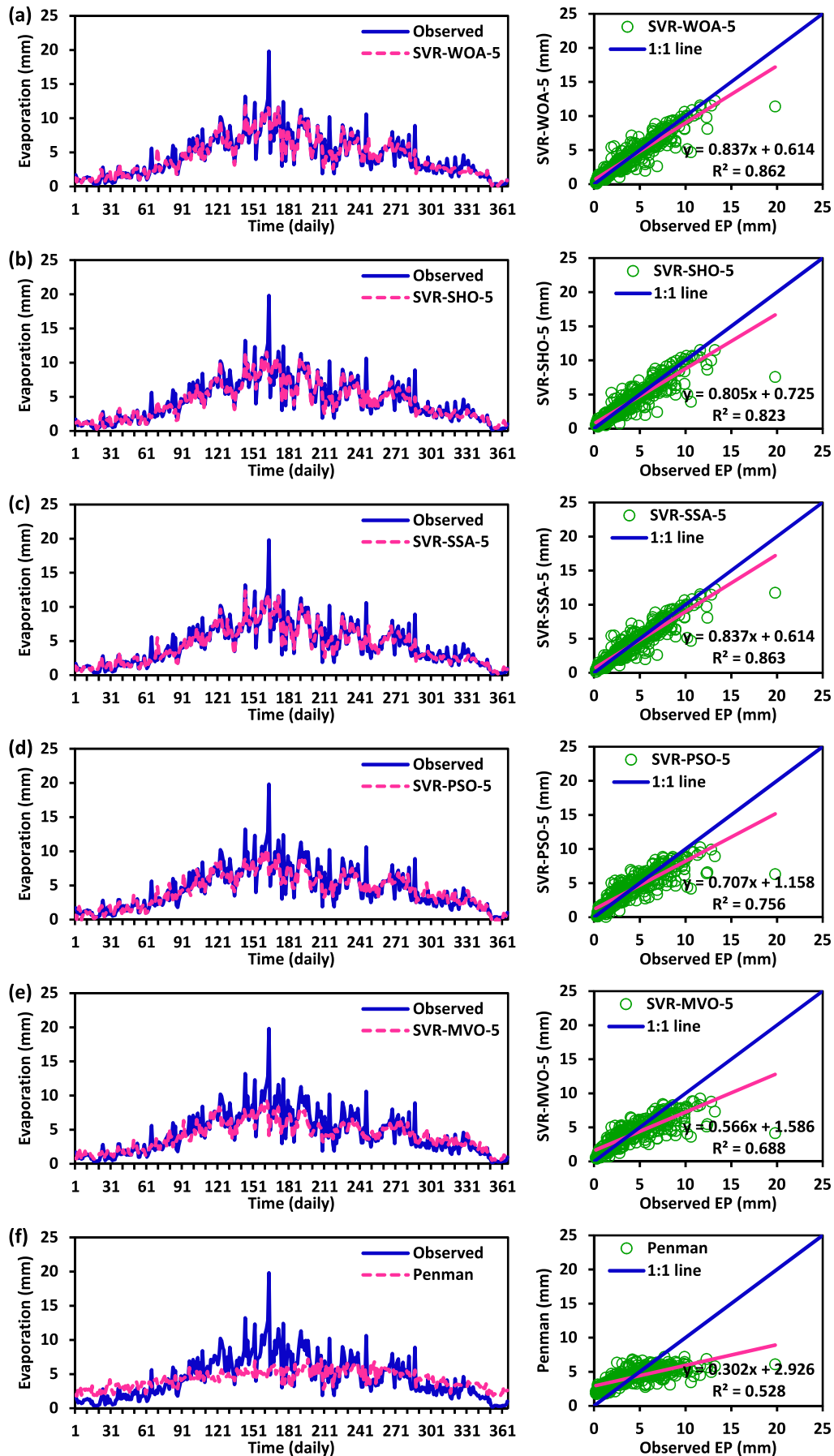


Figure 5. Observed vs estimated daily EP values by the SVR-WOA-5, SVR-SHO-5, SVR-SSA-5, SVR-PSO-5, SVR-MVO-5, and PM models during testing at Hisar station.

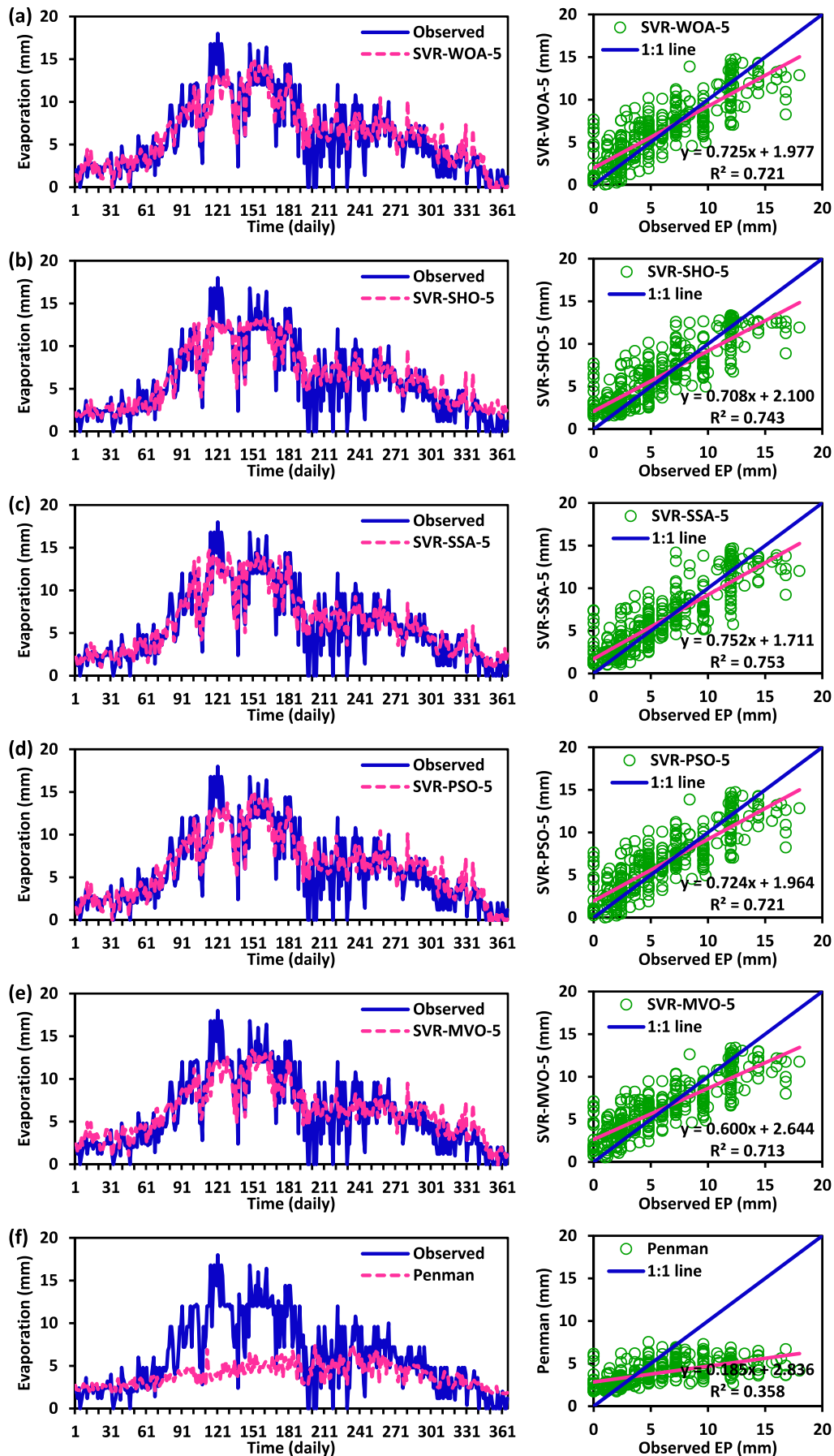


Figure 6. Observed vs estimated daily EP values by the SVR-WOA-5, SVR-SHO-5, SVR-SSA-5, SVR-PSO-5, SVR-MVO-5, and PM models during testing at Bathinda station.

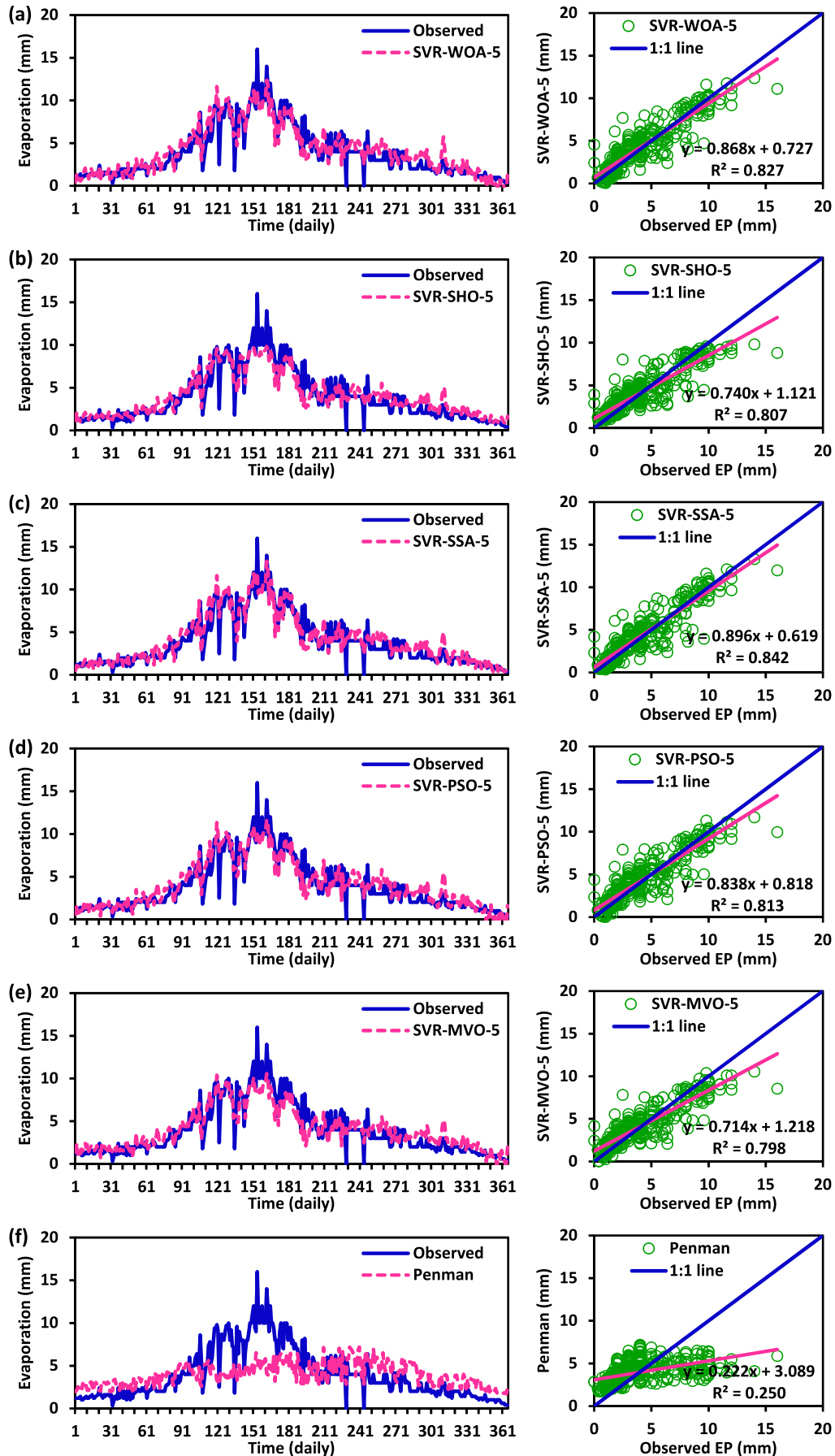


Figure 7. Observed vs estimated daily EP values by the SVR-WOA-5, SVR-SHO-5, SVR-SSA-5, SVR-PSO-5, SVR-MVO-5, and PM models during testing at Ludhiana station.

observed at Bathinda compared to the other two locations due to noisy data, as mentioned earlier. The lower R^2 values for the Penman method at Hisar, Bathinda, and Ludhiana stations indicate the very high efficiency of hybrid models used in this study compared to the conventional EP estimation method. The comparison of the performance of the hybrid models based on scatter plots revealed the better performance of hybrid SVR-SSA-5 compared to the other four hybrids and one conventional model at Hisar, Bathinda, and Ludhiana.

The underestimations of high EP values by all the hybrid models were also noticed in scatter plots for all the stations. Overestimations of low EP values were also clearly visible from the scatter plot at Bathinda station

(Figure 6). Here, it should be noted that EP depends on complex interactions of multiple meteorological variables, including wind speed and temperature, which fluctuate very rapidly on a daily scale. This makes the daily EP time series highly random, which is very difficult to predict accurately (Majhi & Naidu, 2021; Yaseen et al., 2020a). The present study revealed that the SVR model optimized using different nature-inspired algorithms can estimate the daily EP reliably (Allawi et al., 2020; Guan et al., 2020).

Finally, the Taylor diagram (Taylor, 2001) was employed to evaluate the performance of different hybrid models and the Penman model. Figure 8(a-c) demonstrates the results at three stations. In these figures, the

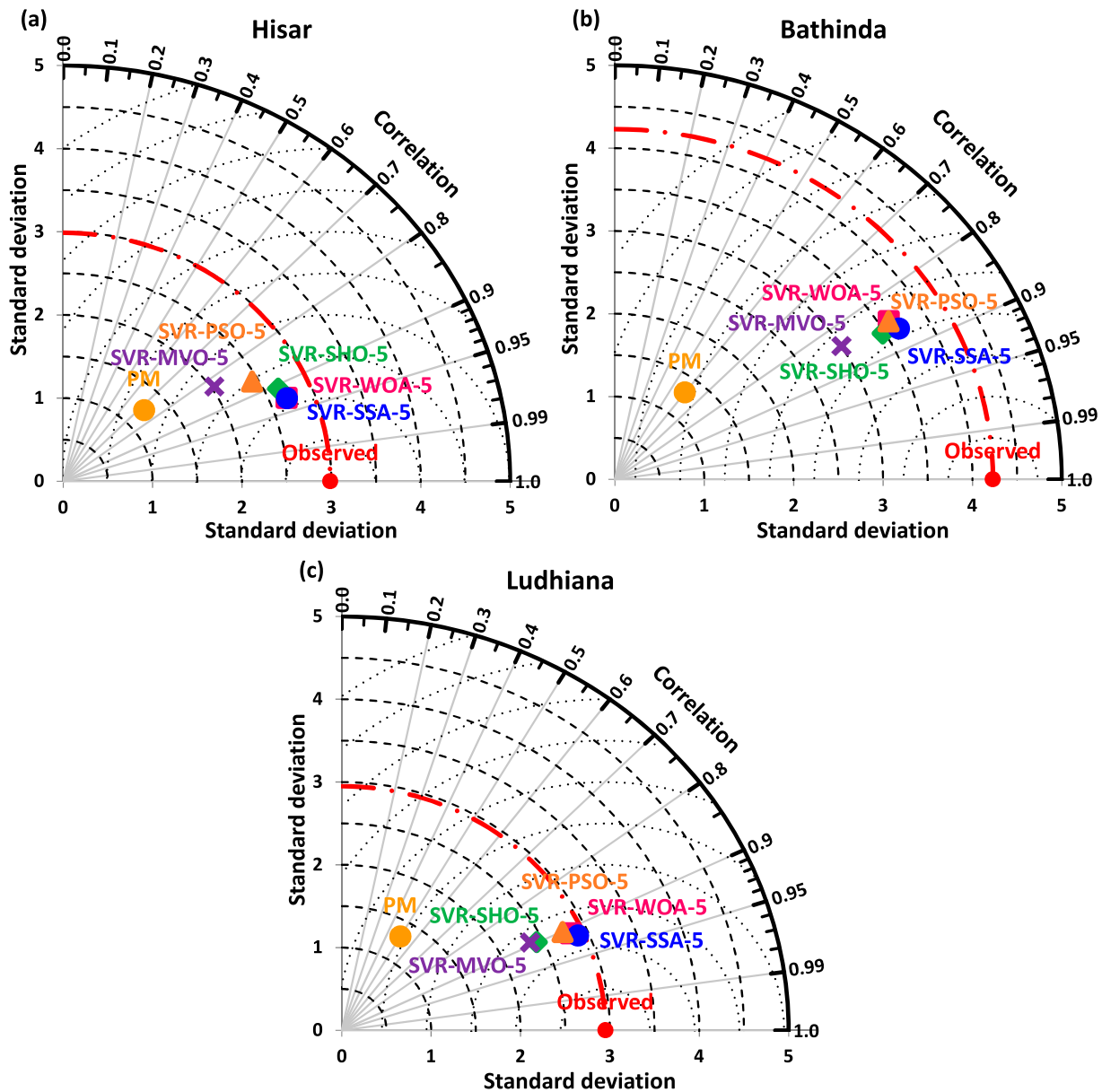


Figure 8. Taylor diagrams of SVR-WOA-5, SVR-SHO-5, SVR-SSA-5, SVR-PSO-5, SVR-MVO-5, and PM models in the testing phase at (a) Hisar (b) Bathinda, and (c) Ludhiana stations.

observed EP is characterized by a red-filled circle (x-axis). Generally, three statistics including correlation coefficient, standard deviation, and RMSE are comprised in the polar system for truthful evaluation of the comparative performance of different models (Ashrafzadeh et al., 2019; Taylor, 2001). The Taylor diagrams show the very close efficacy of hybrid SVR models on Hisar (Figure 8a). The models were clustered very close to each other and near the observed point in the Taylor diagram, indicating the very close performance of the models at this location. At Bathinda (Figure 8b), SVR-SSA-5 showed a higher performance compared to the other four hybrid SVR models and one conventional model. The standard deviation (SD) of the SVR-SSA-5 estimated EP was exactly the same as the observed EP, indicating a perfect performance of the SVR-SSA-5 model. The SVR-SSA-5 model also performed better than the other four hybrid models and one conventional model at Ludhiana (Figure 8c). The SVR-SSA-5 also showed very close to the observed SD of EP at this station. The performance of the Penman method was found unsatisfactory at all the stations. It showed a very low SD compared to the observed SD, which means it cannot estimate the daily variability of EP in the study area.

4.3. Discussion

In this study, daily pan evaporation was estimated from six meteorological variables, T_{\min} , T_{\max} , RH_{\max} , RH_{\min} , U_s , and R_s . Pan-evaporation is the evaporation from an open water body. It depends on the integrated effect of radiation, air temperature, air humidity, and wind on evapotranspiration (Majhi & Naidu, 2021; Wang et al., 2017). Solar radiation provides the necessary energy for water to evaporate. Therefore, it is the most important factor of EP in most parts of the world (Muhammad et al., 2019). The energy needed for evaporation decreases with the increase of temperature. Low air humidity or less water vapor in the air allows more evaporation. Higher wind speed sweeps away more water from the water-body to the atmosphere (Chu et al., 2012). Therefore, all these climatic factors significantly influence EP in any region. Muhammad et al. (2019) used EP as a proxy of evapotranspiration (ET) to evaluate the performance of 31 empirical ET models based on different inputs in peninsular Malaysia. They found only the combination-based model that considers all climatic variables (maximum and minimum temperature, humidity, wind speed, and solar radiation) can reliably estimate ET. This indicates significant impacts of all meteorological factors on EP. Similar results were also reported from different climatic regions of the world (Hounguè et al., 2019; Rodrigues et al., 2020). The present study also found

that all meteorological variables are required for reliable estimation of EP. Therefore, the models were developed in this study using all the available meteorological variables.

The influence of multiple meteorological variables and their interactions makes EP a complex process. Randomness is common in EP data due to the random variability of wind. Besides, outliers are more in EP series due to the coincidence of high temperature and wind with low air humidity events, particularly in dry summer and opposite scenarios during wet winter. These noisy outliers are also often produced by complex interactions of meteorological variables and the influence of the surrounding environment on meteorological variables. Therefore, often not predictable using meteorological variables. For example, the wind speed of an area depends on wind obstructing land use along the wind direction. Therefore, any change in wind direction often causes large variability in localized wind speed and noisy EP. Such noisy EP values are often difficult to predict using meteorological variables. This has been noticed for Bathinda station, where none of the models could estimate high EP values.

The results of this study were compared with the previous studies conducted on modeling pan-evaporation using several artificial intelligence (AI) techniques optimized by bio-inspired algorithms (Kumar et al., 2021; Majhi et al., 2020; Qasem et al., 2019; Salih et al., 2019; Singh et al., 2021). The previous studies reported the effective utility of hybrid AI methods for pan-evaporation at different locations in varying climates through statistical metrics and visual investigation. Ashrafzadeh et al. (2019) estimated the daily evaporation from two stations situated in the northern region of Iran by employing the multilayer perceptron-krill herd optimization (MLP-KHO), MLP, and SVM models. The results indicate the better performance of MLP-KHO model with $R^2 = 0.907, 0.931$, $RMSE = 0.725, 0.855$ mm/day, $IOA = 0.942, 0.950$, and $NSE = 0.789$ and 0.813 for both study stations than the other models. Wu et al. (2020) used the two-hybrid ELMs, embedded with flower pollination algorithm (ELM-FPA) and WOA (ELM-WOA), and evaluated their performance against the differential evolution algorithm-ELM (DEA-ELM), improved M5 tree (M5P) and ANN in predicting monthly pan-evaporation at four weather stations located in the Poyang lake basin of southern China. They found that the hybrid ELM-FPA model attains the highest prediction accuracy ($RMSE = 0.245, 0.283, 0.299, 0.278$ mm/day, $MAE = 0.123, 0.122, 0.129, 0.126$ mm/day, $R^2 = 0.924, 0.908, 0.905, 0.864$, and $NSE = 0.908, 0.907, 0.903, 0.847$) than the others model for all four locations. Seifi and Soroush (2020) optimized ANN with three

novel meta-heuristic algorithms, including Grey Wolf Optimizer (GWO), WOA, and GA, for estimating the daily pan-evaporation in five agro-climatic zones (i.e. hyper-arid, semiarid, arid, humid, and sub-humid) of Iran. The outcomes demonstrate the superior performance of the ANN-GA model ($R^2 = 0.83, 0.79, 0.86, 0.77, 0.69$, RMSE = 0.95, 1.39, 1.98, 1.57, 1.43 mm/day, NSE = 0.82, 0.78, 0.86, 0.77, 0.68) over the other models in all the agro-climatic zones.

The present studies showed better performance of SVR-SSA compared to that obtained using different hybrid ML models in different regions. The NSE and R^2 values for SVR-SSA at Hisar station were 0.861 and 0.929, respectively. It is much higher than that obtained by Seifi and Soroush (2020) using ANN-GWO, ANN-WOA, and ANN-GA models in different climatic regions of Iran. They achieved the highest performance using ANN-GA in the semiarid region ($R^2 = 0.79$ and NSE = 0.78), which is much poorer than that obtained using SVR-SSA in the present study. The SVR-SSA also showed higher performance in R^2 than that found by Wu et al. (2020) using ELM-FPA, ELM-WOA, DEA-ELM, M5P, and ANN. They found the highest $R^2 = 0.924$ for ELM-FPA, which is a bit lower than 0.929, obtained using SVR-SSA in the present study. The results obtained through the exploration of the feasibility of the SSA integrated with SVR for daily pan-evaporation estimation at three study locations in two different agro-climatic zones (i.e. semiarid and sub-humid) establish that the newly constructed hybrid model, i.e. SVR-SSA stands as a robust, reliable, and dynamic optimization method for daily EP estimation.

5. Conclusion

This work aimed to enhance the performance of SVR embedded with a novel meta-heuristic algorithm, i.e. SSA, for estimating daily pan-evaporation (EP) in two different agro-climatic zones of India. The outcomes obtained by the novel SVR-SSA hybrid model were examined against the four-hybrid SVR models (i.e. SVR-MVO, SVR-WOA, SVR-SHO, & SVR-PSO), and one conventional model (i.e. Penman) using the goodness-of-fit and graphical inspection. The most influential input variable combination was demarcated by utilizing the Gamma test (GT) to calibrate and validate the applied hybrid SVR and Penman models at study locations. Evaluation of results demonstrated the superior performance of the novel hybrid SVR-SSA model over other applied models at all study locations. Thus, the SSA algorithm was highly recommended for optimizing SVR model efficacy. Also, the results of the hybrid SVR-SSA approach in conjunction with the Gamma test can help the hydrologists, agronomists, and environmentalists to

construct a smart intelligent system for agricultural practices and sustainable management of water resources for the study locations in two different agro-climatic zones.

Disclosure statement

No potential conflict of interest was reported by the author(s).

ORCID

Anurag Malik  <http://orcid.org/0000-0002-0298-5777>

Shamsuddin Shahid  <http://orcid.org/0000-0001-9621-6452>

Padam Singh  <http://orcid.org/0000-0003-3315-7648>

Saad Shauket Sammen  <http://orcid.org/0000-0002-1708-0612>

References

- Abba, S. I., Abdulkadir, R. A., Gaya, M. S., Sammen, S. S., Ghali, U., Nawaila, M. B., Oğuz, G., Malik, A., & Al-Ansari, N. (2021). Effluents quality prediction by using nonlinear dynamic block-oriented models: A system identification approach. *Desalination and Water Treatment*, 218, 52–62. <https://doi.org/10.5004/dwt.2021.26983>
- Al-Zoubi, A. M., Faris, H., Alqatawna, J., & Hassonah, M. A. (2018). Evolving support vector machines using whale optimization algorithm for spam profiles detection on online social networks in different lingual contexts. *Knowledge-Based Systems*, 153, 91–104. <https://doi.org/10.1016/j.knsys.2018.04.025>
- Aljarah, I., Mafarja, M., Heidari, A. A., Faris, H., & Mirjalili, S. (2020). Multi-verse Optimizer: Theory, Literature Review, and Application in Data Clustering. In *Studies in Computational Intelligence* (pp. 123–141). https://doi.org/10.1007/978-3-030-12127-3_8.
- Allawi, M. F., Aidan, I. A., & El-Shafie, A. (2020). Enhancing the performance of data-driven models for monthly reservoir evaporation prediction. *Environmental Science and Pollution Research*, 28(7), 8281–8295. <https://doi.org/10.1007/s11356-020-11062-x>
- Allen, R. G., Pereira, L. S., Raes, D., & Smith, M. (1998). Crop evapotranspiration: Guidelines for computing crop requirements FAO Irrig. Drain. Pap, 56. FAO, ROME, 300(9), D05109.
- Ashrafzadeh, A., Ghorbani, M. A., Biazar, S. M., & Yaseen, Z. M. (2019). Evaporation process modelling over northern Iran: Application of an integrative data-intelligence model with the krill herd optimization algorithm. *Hydrological Sciences Journal*, 64(15), 1843–1856. <https://doi.org/10.1080/0262667.2019.1676428>
- Ashrafzadeh, A., Malik, A., Jothiprakash, V., Ghorbani, M. A., & Biazar, S. M. (2020). Estimation of daily pan evaporation using neural networks and meta-heuristic approaches. *ISH Journal of Hydraulic Engineering*, 26(4), 421–429. <https://doi.org/10.1080/09715010.2018.1498754>
- Azorin-Molina, C., Vicente-Serrano, S. M., Sanchez-Lorenzo, A., McVicar, T. R., Morán-Tejeda, E., Revuelto, J., El Kenawy, A., Martín-Hernández, N., & Tomas-Burguera, M. (2015). Atmospheric evaporative demand observations, estimates and driving factors in Spain (1961–2011). *Journal of Hydrology*, 523, 262–277. <https://doi.org/10.1016/j.jhydrol.2015.01.046>

- Borji, M., Malekian, A., Salajegheh, A., & Ghadimi, M. (2016). Multi-time-scale analysis of hydrological drought forecasting using support vector regression (SVR) and artificial neural networks (ANN). *Arabian Journal of Geosciences*, 9(19), 725. <https://doi.org/10.1007/s12517-016-2750-x>
- Burn, D. H., & Hesch, N. M. (2007). Trends in evaporation for the Canadian Prairies. *Journal of Hydrology*, 336(1-2), 61–73. <https://doi.org/10.1016/j.jhydrol.2006.12.011>
- Choubin, B., & Malekian, A. (2017). Combined gamma and M-test-based ANN and ARIMA models for groundwater fluctuation forecasting in semiarid regions. *Environmental Earth Sciences*, 76(15), 1–10. <https://doi.org/10.1007/s12665-017-6870-8>
- Chu, C. R., Li, M. H., Chang, Y. F., Liu, T. C., & Chen, Y. Y. (2012). Wind-induced splash in Class A evaporation pan. *Journal of Geophysical Research: Atmospheres*, 117(D11). <https://doi.org/10.1029/2011JD016848>
- Cui, F., Salih, S. Q., Choubin, B., Bhagat, S. K., Samui, P., & Yaseen, Z. M. (2020). Newly explored machine learning model for river flow time series forecasting at Mary River, Australia. *Environmental Monitoring and Assessment*, 192(12). <https://doi.org/10.1007/s10661-020-08724-1>
- Das, B. S., Devi, K., & Khatua, K. K. (2019). Prediction of discharge in converging and diverging compound channel by gene expression programming. *ISH Journal of Hydraulic Engineering*, 1–11. <https://doi.org/10.1080/09715010.2018.1558116>
- Dhiman, G., & Kumar, V. (2017). Spotted hyena optimizer: A novel bio-inspired based metaheuristic technique for engineering applications. *Advances in Engineering Software*, 114, 48–70. <https://doi.org/10.1016/j.advengsoft.2017.05.014>
- Dhiman, G., & Kumar, V. (2019). Spotted hyena optimizer for solving complex and non-linear constrained engineering problems. *Advances in Intelligent Systems and Computing*, 741, 857–867. https://doi.org/10.1007/978-981-13-0761-4_81
- Elaziz, M. A., & Mirjalili, S. (2019). A hyper-heuristic for improving the initial population of whale optimization algorithm. *Knowledge-Based Systems*, 172, 42–63. <https://doi.org/10.1016/j.knsys.2019.02.010>
- Elbeltagi, A., Deng, J., Wang, K., Malik, A., & Maroufpoor, S. (2020). Modeling long-term dynamics of crop evapotranspiration using deep learning in a semi-arid environment. *Agricultural Water Management*, 241, 106334. <https://doi.org/10.1016/j.agwat.2020.106334>
- Feng, Y., Jia, Y., Zhang, Q., Gong, D., & Cui, N. (2018). National-scale assessment of pan evaporation models across different climatic zones of China. *Journal of Hydrology*, 564, 314–328. <https://doi.org/10.1016/j.jhydrol.2018.07.013>
- Ghaemi, A., Rezaie-Balf, M., Adamowski, J., Kisi, O., & Quilty, J. (2019). On the applicability of maximum overlap discrete wavelet transform integrated with MARS and M5 model tree for monthly pan evaporation prediction. *Agricultural and Forest Meteorology*, 278, 107647. <https://doi.org/10.1016/j.agrformet.2019.107647>
- Ghorbani, M. A., Kazempour, R., Chau, K.-W., Shamshirband, S., & Ghazvinei, P. T. (2018). Forecasting pan evaporation with an integrated artificial neural network quantum-behaved particle swarm optimization model: A case study in Talesh, Northern Iran. *Engineering Applications of Computational Fluid Mechanics*, 12, 724–737. <https://doi.org/10.1080/19942060.2018.1517052>
- Guan, Y., Mohammadi, B., Pham, Q. B., Adarsh, S., Balkhair, K. S., Rahman, K. U., Linh, N. T. T., & Tri, D. Q. (2020). A novel approach for predicting daily pan evaporation in the coastal regions of Iran using support vector regression coupled with krill herd algorithm model. *Theoretical and Applied Climatology*, 142(1-2), 349–367. <https://doi.org/10.1007/s00704-020-03283-4>
- Gunn, S. (1998). Support vector machines for classification and regression. Image Speech Intell. Syst. Res. Group, Univ. Southapt.
- Heidari, A. A., Aljarah, I., Faris, H., Chen, H., Luo, J., & Mirjalili, S. (2020). An enhanced associative learning-based exploratory whale optimizer for global optimization. *Neural Computing and Applications*, 32(9), 5185–5211. <https://doi.org/10.1007/s00521-019-04015-0>
- Hounguè, R., Lawin, A. E., Moumouni, S., & Afouda, A. A. (2019). Change in climate extremes and pan evaporation influencing factors over Ouémé Delta in Bénin. *Climate*, 7(1). <https://doi.org/10.3390/cli7010002>
- Jajarmizadeh, M., Kakaei Lafdani, E., Harun, S., & Ahmadi, A. (2015). Application of SVM and SWAT models for monthly streamflow prediction, a case study in South of Iran. *KSCSE Journal of Civil Engineering*, 19(1), 345–357. <https://doi.org/10.1007/s12205-014-0060-y>
- Kakaei Lafdani, E., Moghaddam Nia, A., & Ahmadi, A. (2013). Daily suspended sediment load prediction using artificial neural networks and support vector machines. *Journal of Hydrology*, 478, 50–62. <https://doi.org/10.1016/j.jhydrol.2012.11.048>
- Keerthi, S. S., & Lin, C. J. (2003). Asymptotic behaviors of support vector machines with Gaussian kernel. *Neural Computation*, 15(7), 1667–1689. <https://doi.org/10.1162/089976603321891855>
- Kennedy, J., & Eberhart, R. (1995). Proceedings of ICNN'95 – International Conference on Neural Networks. In: Particle Swarm Optimization.
- Keshtegar, B., Heddami, S., Sebban, A., Zhu, S. P., & Trung, N. T. (2019). SVR-RSM: A hybrid heuristic method for modeling monthly pan evaporation. *Environmental Science and Pollution Research*, 26(35), 35807–35826. <https://doi.org/10.1007/s11356-019-06596-8>
- Kim, S., Shiri, J., Singh, V. P., Kisi, O., & Landaras, G. (2015). Predicting daily pan evaporation by soft computing models with limited climatic data. *Hydrological Sciences Journal*, 60(6), 1120–1136. <https://doi.org/10.1080/02626667.2014.945937>
- Kisi, O., & Heddami, S. (2019). Evaporation modelling by heuristic regression approaches using only temperature data. *Hydrological Sciences Journal*, 64(6), 653–672. <https://doi.org/10.1080/02626667.2019.1599487>
- Kumar, M., Kumari, A., Kumar, D., Al-Ansari, N., Ali, R., Kumar, R., Kumar, A., Elbeltagi, A., & Kuriqi, A. (2021). The superiority of data-driven techniques for estimation of daily pan evaporation. *Atmosphere*, 12(6), 701. <https://doi.org/10.3390/atmos12060701>
- Majhi, B., & Naidu, D. (2021). Pan evaporation modeling in different agroclimatic zones using functional link artificial neural network. *Information Processing in Agriculture*, 8, 134–147. <https://doi.org/10.1016/j.inpa.2020.02.007>
- Majhi, B., Naidu, D., Mishra, A. P., & Satapathy, S. C. (2020). Improved prediction of daily pan evaporation using deep-LSTM model. *Neural Computing and Applications*,

- 32(12), 7823–7838. <https://doi.org/10.1007/s00521-019-04127-7>
- Majidi, M., Alizadeh, A., Farid, A., & Vazifedoust, M. (2015). Estimating evaporation from lakes and reservoirs under limited data condition in a semi-arid region. *Water Resources Management*, 29(10), 3711–3733. <https://doi.org/10.1007/s11269-015-1025-8>
- Malik, A., Kumar, A., Ghorbani, M. A., Kashani, M. H., Kisi, O., & Kim, S. (2019). The viability of co-active fuzzy inference system model for monthly reference evapotranspiration estimation: Case study of Uttarakhand state. *Hydrology Research*, 50(6), 1623–1644. <https://doi.org/10.2166/nh.2019.059>
- Malik, A., Kumar, A., Kim, S., Kashani, M. H., Karimi, V., Sharafati, A., Ghorbani, M. A., Al-Ansari, N., Salih, S. Q., Yaseen, Z. M., & Chau, K.-W. (2020a). Modeling monthly pan evaporation process over the Indian central Himalayas: Application of multiple learning artificial intelligence model. *Engineering Applications of Computational Fluid Mechanics*, 14, 323–338. <https://doi.org/10.1080/19942060.2020.1715845>
- Malik, A., Kumar, A., & Kisi, O. (2017). Monthly pan evaporation estimation in Indian central Himalayas using different heuristic approaches and climate based models. *Computers and Electronics in Agriculture*, 143, 302–313. <https://doi.org/10.1016/j.compag.2017.11.008>
- Malik, A., Kumar, A., & Kisi, O. (2018). Daily pan evaporation estimation using heuristic methods with gamma test. *Journal of Irrigation and Drainage Engineering*, 144(9), 04018023. [https://doi.org/10.1061/\(ASCE\)IR.1943-4774.0001336](https://doi.org/10.1061/(ASCE)IR.1943-4774.0001336)
- Malik, A., Kumar, A., Pham, Q. B., Zhu, S., Linh, N. T. T., & Tri, D. Q. (2020b). Identification of EDI trend using Mann-Kendall and sen-innovative trend methods (Uttarakhand, India). *Arabian Journal of Geosciences*, 13(18), 951. <https://doi.org/10.1007/s12517-020-05926-2>
- Malik, A., Rai, P., Heddami, S., Kisi, O., Sharafati, A., Salih, S. Q., Al-Ansari, N., & Yaseen, Z. M. (2020c). Pan evaporation estimation in Uttarakhand and Uttar Pradesh states, India: Validity of an integrative data intelligence model. *Atmosphere*, 11, 1–26. <https://doi.org/10.3390/atmos11060553>
- Malik, A., Tikhamarine, Y., Sammen, S. S., Abba, S. I., & Shahid, S. (2021a). Prediction of meteorological drought by using hybrid support vector regression optimized with HHO versus PSO algorithms. *Environmental Science and Pollution Research*. <https://doi.org/10.1007/s11356-021-13445-0>
- Malik, A., Tikhamarine, Y., Souag-Gamane, D., Kisi, O., & Pham, Q. B. (2020d). Support vector regression optimized by meta-heuristic algorithms for daily streamflow prediction. *Stochastic Environmental Research and Risk Assessment*, 34(11), 1755–1773. <https://doi.org/10.1007/s00477-020-01874-1>
- Malik, A., Tikhamarine, Y., Souag-Gamane, D., Rai, P., Sammen, S. S., & Kisi, O. (2021b). Support vector regression integrated with novel meta-heuristic algorithms for meteorological drought prediction. *Meteorology and Atmospheric Physics*, 133(3), 891–909. <https://doi.org/10.1007/s00703-021-00787-0>
- Mirjalili, S., Gandomi, A. H., Mirjalili, S. Z., Saremi, S., Faris, H., & Mirjalili, S. M. (2017). Salp swarm algorithm: A bio-inspired optimizer for engineering design problems. *Advances in Engineering Software*, 114, 163–191. <https://doi.org/10.1016/j.advengsoft.2017.07.002>
- Mirjalili, S., & Lewis, A. (2016). The whale optimization algorithm. *Advances in Engineering Software*, 95, 51–67. <https://doi.org/10.1016/j.advengsoft.2016.01.008>
- Mirjalili, S., Mirjalili, S. M., & Hatamlou, A. (2016). Multi-verse optimizer: A nature-inspired algorithm for global optimization. *Neural Computing and Applications*, 27(2), 495–513. <https://doi.org/10.1007/s00521-015-1870-7>
- Mirjalili, S., Mirjalili, S. M., Saremi, S., & Mirjalili, S. (2020). Whale optimization algorithm: Theory, literature review, and application in designing photonic crystal filters. *Studies in Computational Intelligence*, 811, 219–238. https://doi.org/10.1007/978-3-030-12127-3_13
- Moazenzadeh, R., Mohammadi, B., Shamshirband, S., & Chau, K. W. (2018). Coupling a firefly algorithm with support vector regression to predict evaporation in northern Iran. *Engineering Applications of Computational Fluid Mechanics*, 12(1), 584–597. <https://doi.org/10.1080/19942060.2018.1482476>
- Mohammadi, A. A., Yousefi, M., Soltani, J., Ahangar, A. G., & Javan, S. (2018). Using the combined model of gamma test and neuro-fuzzy system for modeling and estimating lead bonds in reservoir sediments. *Environmental Science and Pollution Research*, 25(30), 30315–30324. <https://doi.org/10.1007/s11356-018-3026-7>
- Muhammad, M. K. I., Nashwan, M. S., Shahid, S., Ismail, T. B., Song, Y. H., & Chung, E. S. (2019). Evaluation of empirical reference evapotranspiration models using compromise programming: A case study of Peninsular Malaysia. *Sustainability*, 11(16). <https://doi.org/10.3390/su11164267>
- Nash, J. E., & Sutcliffe, J. V. (1970). River flow forecasting through conceptual models part I – A discussion of principles. *Journal of Hydrology*, 10(3), 282–290. [https://doi.org/10.1016/0022-1694\(70\)90255-6](https://doi.org/10.1016/0022-1694(70)90255-6)
- Panahi, M., Sadhasivam, N., Pourghasemi, H. R., Rezaie, F., & Lee, S. (2020). Spatial prediction of groundwater potential mapping based on convolutional neural network (CNN) and support vector regression (SVR). *Journal of Hydrology*, 588, 125033. <https://doi.org/10.1016/j.jhydrol.2020.125033>
- Pandey, K., Kumar, S., Malik, A., & Kuriqi, A. (2020). Artificial neural network optimized with a genetic algorithm for seasonal groundwater table depth prediction in Uttar Pradesh, India. *Sustainability*, 12(21). <https://doi.org/10.3390/su12218932>
- Patle, G. T., Chettri, M., & Jhahharia, D. (2020). Monthly pan evaporation modelling using multiple linear regression and artificial neural network techniques. *Water Supply*, 20(3), 800–808. <https://doi.org/10.2166/ws.2019.189>
- Penman, H. L. (1948). Natural evaporation from open water, bare soil and grass. *Proceedings of the Royal Society of London. Series A. Mathematical and Physical Sciences*, 193(1032), 120–145. <https://doi.org/10.1098/rspa.1948.0037>
- Penman, H. L. (1956). Evaporation: An introductory survey. *NJAS Wageningen Journal of Life Sciences*, 4(1), 9–29.
- Piri, J., Amin, S., Moghaddamnia, A., Keshavarz, A., Han, D., & Remesan, R. (2009). Daily pan evaporation modeling in a hot and dry climate. *Journal of Hydrologic Engineering*, 14(8), 803–811. [https://doi.org/10.1061/\(ASCE\)HE.1943-5584.0000056](https://doi.org/10.1061/(ASCE)HE.1943-5584.0000056)
- Pour, S. H., Wahab, A. K. A., Shahid, S., & Ismail, Z. B. (2020). Changes in reference evapotranspiration and its driving factors in peninsular Malaysia. *Atmospheric Research*, 246. <https://doi.org/10.1016/j.atmosres.2020.105096>

- Qasem, S. N., Samadianfard, S., Kheshtgar, S., Jarhan, S., Kisi, O., Shamshirband, S., & Chau, K.-W. (2019). Modeling monthly pan evaporation using wavelet support vector regression and wavelet artificial neural networks in arid and humid climates. *Engineering Applications of Computational Fluid Mechanics*, 13, 177–187. <https://doi.org/10.1080/19942060.2018.1564702>
- Rashidi, S., Vafakhah, M., Lafdani, E. K., & Javadi, M. R. (2016). Evaluating the support vector machine for suspended sediment load forecasting based on gamma test. *Arabian Journal of Geosciences*, 9(11), 1–15. <https://doi.org/10.1007/s12517-016-2601-9>
- Rehamnia, I., Benlaoukli, B., Jamei, M., Karbasi, M., & Malik, A. (2021). Simulation of seepage flow through embankment dam by using a novel extended Kalman filter based neural network paradigm: Case study of Fontaine Gazelles Dam, Algeria. *Measurement*, 176, 109219. <https://doi.org/10.1016/j.measurement.2021.109219>
- Rezaie-Balf, M., Kisi, O., & Chua, L. H. C. (2019). Application of ensemble empirical mode decomposition based on machine learning methodologies in forecasting monthly pan evaporation. *Hydrology Research*, 50(2), 498–516. <https://doi.org/10.2166/nh.2018.050>
- Rodrigues, C. M., Moreira, M., Guimaraes, R. C., & Potes, M. (2020). Reservoir evaporation in a Mediterranean climate: Comparing direct methods in Alqueva Reservoir, Portugal. *Hydrology and Earth System Sciences*, 24(12), 5973–5984. <https://doi.org/10.5194/hess-24-5973-2020>
- Salih, S. Q., Allawi, M. F., Yousif, A. A., Armanuos, A. M., Saggi, M. K., Ali, M., Shahid, S., Al-Ansari, N., Yaseen, Z. M., & Chau, K.-W. (2019). Viability of the advanced adaptive neuro-fuzzy inference system model on reservoir evaporation process simulation: Case study of Nasser Lake in Egypt. *Engineering Applications of Computational Fluid Mechanics*, 13(1), 878–891. <https://doi.org/10.1080/19942060.2019.1647879>
- Sebbar, A., Heddami, S., & Djemili, L. (2019). Predicting daily pan evaporation (Epan) from dam reservoirs in the mediterranean regions of Algeria: OPELM vs OSELM. *Environmental Processes*, 6(1), 309–319. <https://doi.org/10.1007/s40710-019-00353-2>
- Seifi, A., & Riahi, H. (2020). Estimating daily reference evapotranspiration using hybrid gamma test-least square support vector machine, gamma test-ANN, and gamma test-ANFIS models in an arid area of Iran. *Journal of Water and Climate Change*, 11(1), 217–240. <https://doi.org/10.2166/wcc.2018.003>
- Seifi, A., & Soroush, F. (2020). Pan evaporation estimation and derivation of explicit optimized equations by novel hybrid meta-heuristic ANN based methods in different climates of Iran. *Computers and Electronics in Agriculture*, 173. <https://doi.org/10.1016/j.compag.2020.105418>
- Shabani, S., Samadianfard, S., Sattari, M. T., Mosavi, A., Shamshirband, S., Kmet, T., & Várkonyi-Kóczy, A. R. (2020). Modeling Pan evaporation using Gaussian process regression K-nearest neighbors random Forest and support vector machines; comparative analysis. *Atmosphere*, 11(1), 66. <https://doi.org/10.3390/atmos11010066>
- Shiri, J., Marti, P., & Singh, V. P. (2014). Evaluation of gene expression programming approaches for estimating daily evaporation through spatial and temporal data scanning. *Hydrological Processes*, 28(3), 1215–1225. <https://doi.org/10.1002/hyp.9669>
- Singh, A., Malik, A., Kumar, A., & Kisi, O. (2018). Rainfall-runoff modeling in hilly watershed using heuristic approaches with gamma test. *Arabian Journal of Geosciences*, 11(1), 1–12. <https://doi.org/10.1007/s12517-018-3614-3>
- Singh, A., Singh, R. M., Kumar, A. R. S., Kumar, A., Hanwat, S., & Tripathi, V. K. (2021). Evaluation of soft computing and regression-based techniques for the estimation of evaporation. *Journal of Water and Climate Change*, 12(1), 32–43. <https://doi.org/10.2166/wcc.2019.101>
- Smola, J., & Scholkopf, B. (1998). A tutorial on support vector regression. R. Hollow. Coll, NeuroCOLT Tech, Technical Rep. Ser.
- Stefánsson, A., Končar, N., & Jones, A. J. (1997). A note on the gamma test. *Neural Computing & Applications*, 5(3), 131–133. <https://doi.org/10.1007/BF01413858>
- Su, T., Feng, T., & Feng, G. (2015). Evaporation variability under climate warming in five reanalyses and its association with pan evaporation over China. *Journal of Geophysical Research: Atmospheres*, 120(16), 8080–8098. <https://doi.org/10.1002/2014JD023040>
- Tao, H., Diop, L., Bodian, A., Djaman, K., Ndiaye, P. M., & Yaseen, Z. M. (2018). Reference evapotranspiration prediction using hybridized fuzzy model with firefly algorithm: Regional case study in Burkina Faso. *Agricultural Water Management*, 208, 140–151. <https://doi.org/10.1016/j.agwat.2018.06.018>
- Taylor, K. E. (2001). Summarizing multiple aspects of model performance in a single diagram. *Journal of Geophysical Research: Atmospheres*, 106(D7), 7183–7192. <https://doi.org/10.1029/2000JD900719>
- Tharwat, A., & Hassanien, A. E. (2018). Chaotic antlion algorithm for parameter optimization of support vector machine. *Applied Intelligence*, 48(3), 670–686. <https://doi.org/10.1007/s10489-017-0994-0>
- Tikhmarine, Y., Malik, A., Kumar, A., Souag-Gamane, D., & Kisi, O. (2019). Estimation of monthly reference evapotranspiration using novel hybrid machine learning approaches. *Hydrological Sciences Journal*, 64(15), 1824–1842. <https://doi.org/10.1080/02626667.2019.1678750>
- Tikhmarine, Y., Malik, A., Souag-Gamane, D., & Kisi, O. (2020). Artificial intelligence models versus empirical equations for modeling monthly reference evapotranspiration. *Environmental Science and Pollution Research*, 27(24), 30001–30019. <https://doi.org/10.1007/s11356-020-08792-3>
- Vapnik, V. N. (1995). *The nature of statistical learning theory* (p. 314). Springer.
- Wang, L., Kisi, O., Zounemat-Kermani, M., & Li, H. (2017). Pan evaporation modeling using six different heuristic computing methods in different climates of China. *Journal of Hydrology*, 544, 407–427. <https://doi.org/10.1016/j.jhydrol.2016.11.059>
- Wang, J., Wang, Q., Zhao, Y., Li, H., Zhai, J., & Shang, Y. (2015). Temporal and spatial characteristics of pan evaporation trends and their attribution to meteorological drivers in the three-river source region, China. *Journal of Geophysical Research: Atmospheres*, 120(13), 6391–6408. <https://doi.org/10.1002/2014JD022874>
- Wang, T., Zhang, J., Sun, F., & Liu, W. (2017). Pan evaporation paradox and evaporative demand from the past to the future over China: A review. *Wiley Interdisciplinary Reviews: Water*, 4(3), e1207. <https://doi.org/10.1002/wat2.1207>

- Willmott, C. J. (1981). On the validation of models. *Physical Geography*, 2(2), 184–194. <https://doi.org/10.1080/02723646.1981.10642213>
- Wu, L., Huang, G., Fan, J., Ma, X., Zhou, H., & Zeng, W. (2020). Hybrid extreme learning machine with meta-heuristic algorithms for monthly pan evaporation prediction. *Computers and Electronics in Agriculture*, 168. <https://doi.org/10.1016/j.compag.2019.105115>
- Yaseen, Z. M., Al-Juboori, A. M., Beyaztas, U., Al-Ansari, N., Chau, K. W., Qi, C., Ali, M., Salih, S. Q., & Shahid, S. (2020a). Prediction of evaporation in arid and semi-arid regions: A comparative study using different machine learning models. *Engineering Applications of Computational Fluid Mechanics*, 14(1), 70–89. <https://doi.org/10.1080/19942060.2019.1680576>
- Yaseen, Z. M., Faris, H., & Al-Ansari, N. (2020b). Hybridized extreme learning machine model with Salp swarm algorithm: A novel predictive model for hydrological application. *Complexity*, 2020, 1–14. <https://doi.org/10.1155/2020/8206245>